Nuclear Engineering and Technology 50 (2018) 462–469

Contents lists available at ScienceDirect

Nuclear Engineering and Technology

journal homepage: www.elsevier.com/locate/net

Original Article

Background reduction by Cu/Pb shielding and efficiency study of NaI(TI) detector

Revink A. Ramadhan [a,*], Khairi M-S. Abdullah [b]

[a] Department of Physics, College of Science, University of Duhok, Zakho str., Duhok 42001, Kurdistan Region, Iraq
[b] Department of Water Resources, College of Engineering, University of Duhok, Zakho str., Duhok 42001, Kurdistan Region, Iraq

ARTICLE INFO

Article history:
Received 7 October 2017
Received in revised form
15 December 2017
Accepted 28 December 2017
Available online 31 January 2018

Keywords:
Copper
Efficiency
Gamma
Lead Shielding
NaI(Tl) Detector
Spectroscopy

ABSTRACT

The background spectrum of a 3″ × 3″ NaI(Tl) well-type scintillation SILENA detector was measured without shielding, in 6 cm thick lead shielding, and with 2 mm thick electrolytic copper covering the detector inside the lead shielding. The relative remaining background of the lead shield lined with copper was found to be ideal for low-level environmental radioactive spectroscopy. The background total count rate in the (20–2160 KeV) was reduced 28.7 times by the lead and 29 times by the Cu + Pb shielding. The effective reduction of background (1.04) by the copper mainly appeared in the energy range from X-ray up to 500 KeV, while for the total energy range the ratio is 1.01 relative to the lead only. In addition, a strong relation between the full-energy peak absolute efficiency and the detector well height was found using gamma-ray isotropic radiation point sources placed inside the detector well. The full-energy peak efficiency at a midpoint of the well (at 2.5 cm) is three times greater than that on the detector surface. The energy calibrations and the resolution of any single energy line are independent of the locations of the gamma source inside or outside of the well.

1. Introduction

At the beginning of the use of radioactive sources in an assortment of fields such as energy, industry, health physics, and environmental applications, nuclear radiation detectors became fundamental tools because radiation is dangerous to health. In radiation measurement, an accurate knowledge of the detector spectral performance is essential [1].

A major aspect of nuclear spectroscopy is minimization of the background radiation not originating from the sample that is being measured. Background radiation comes from naturally occurring or artificially produced radioactive nuclides in the environment or from cosmic sources [2]. The setup for any detector involves the selection of detector shielding to minimize the influence of background radiation. Of all the shielding materials, the most commonly used are Pb and, in some cases, iron. Pb is favored because of its high density (11340 kg/m^3) and high atomic number (Z = 82). In addition, a thin sheet of Cu to cover the detector is essential against X-rays, created from the interaction of radiation from the background and even coming out of the sample with the outer Pb shielding [3].

NaI(Tl) is one of the most widely used gamma spectrometry material; its performance directly depends on its detection efficiency [4], which can vary with the volume and shape of the detector material, the radiation energy, the absorption cross-section in the material, attenuation layers around the detector, and the physical thickness of the detector in the direction of the incident radiation, along with the source to detector distance and geometry [5,6].

A significant advantage of well-type NaI(Tl) crystal is its high counting efficiency, which can be achieved by placing the samples at the bottom of the well. In this position, almost all gamma rays emitted isotropically from the source are intercepted by at least a portion of the crystal [7]. The well-type is very useful in low level activity and very low mass samples, such as environmental air-filter samples [8]. It is also very efficient for low-energy gamma rays [9]. At very high γ-energies, some advantages are lost because the average path length through the crystal is somewhat less when gamma rays are externally incident on a solid crystal. Accordingly, it is necessary to know the efficiencies and resolution of well-type detectors as a function of gamma energy and the variation of the detector crystal efficiency as a function of the well depth [10,11].

In the present work, study of best shielding for an NaI detector against background radiation as well as the X-rays created by the

* Corresponding author.
E-mail address: revink@uod.ac (R.A. Ramadhan).

https://doi.org/10.1016/j.net.2017.12.016
1738-5733/

main shield (Pb) is carried out. The energy and efficiency as well as resolution calibrations of the 3″ × 3″ NaI(Tl) well-type detector are established in various positions from 0.5 to 6 cm height inside the well, moving up in steps of 0.5 cm. Standard sources are used for these purposes.

2. Experimental part

2.1. Construction of Pb shield

The detector is surrounded by a 4π geometry 6 cm thick Pb shield. An additional 2 mm thick shield of electrolytic Cu, covering the detector inside the Pb shield, is added to eliminate or reduce the characteristic fluorescence X-rays produced mainly by the Pb shield.

The construction of the Pb shield is done by designing an iron cylindrical mould of 16 cm inner diameter, 6 cm thickness, 22 cm height, with an upper opening. Commercial Pb rods were bought and melted on the iron cylindrical mould. Overall weight was approximately 148 kg.

The open, upper Pb cylinder is covered by a central lid surrounded by a ring; the cylinder and ring both are of 6 cm thickness and have masses of 10 and 18 kg, respectively. These lids are made in two parts, for easy opening by hand, not mechanically.

Fig. 1. Setup gamma ray spectrometer, (A) The 3″ ×3″ well-type NaI(Tl) detector with photomultipliers, (B) Cu layers, (C) The opening for samples changing, (D) The photomultipliers passing through the lower part of the shield, (E) Cover shield, (F) The assembled shield.

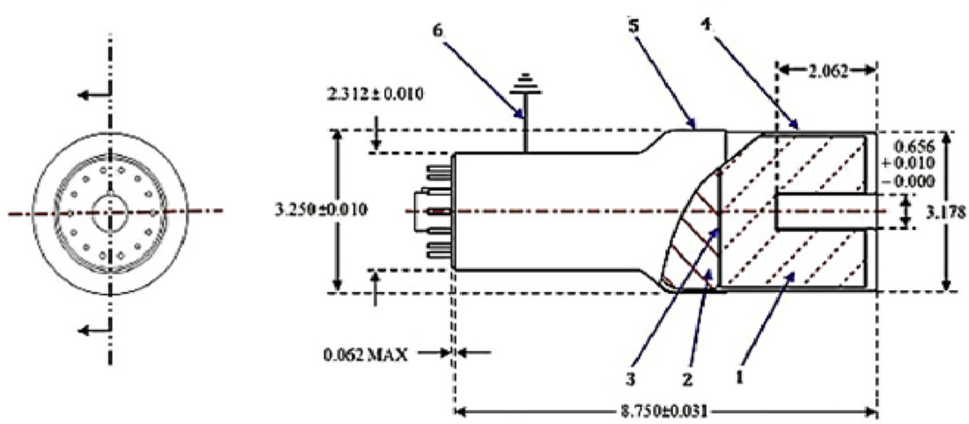

1. Crystal: 3″× 3″ NaI(TI)
2. Photomultiplier tube
3. Bicron proprietary optical coupling
4. Aluminum housing with well: Chrome finish
5. MU-Metal light shield: Chrome finish
6. Light shield grounded to pin 14 (cathode) performances: PHR<9.0% for ^{137}Cs

Energy resolution (FWHM) at 661.6 keV	6.3%
Cathode to anode voltage	820 V dc

Fig. 2. The manufactory diagram of the 3″ × 3″ well-type NaI(Tl) SILENA model 3S3W detector (All dimensions are in inches).

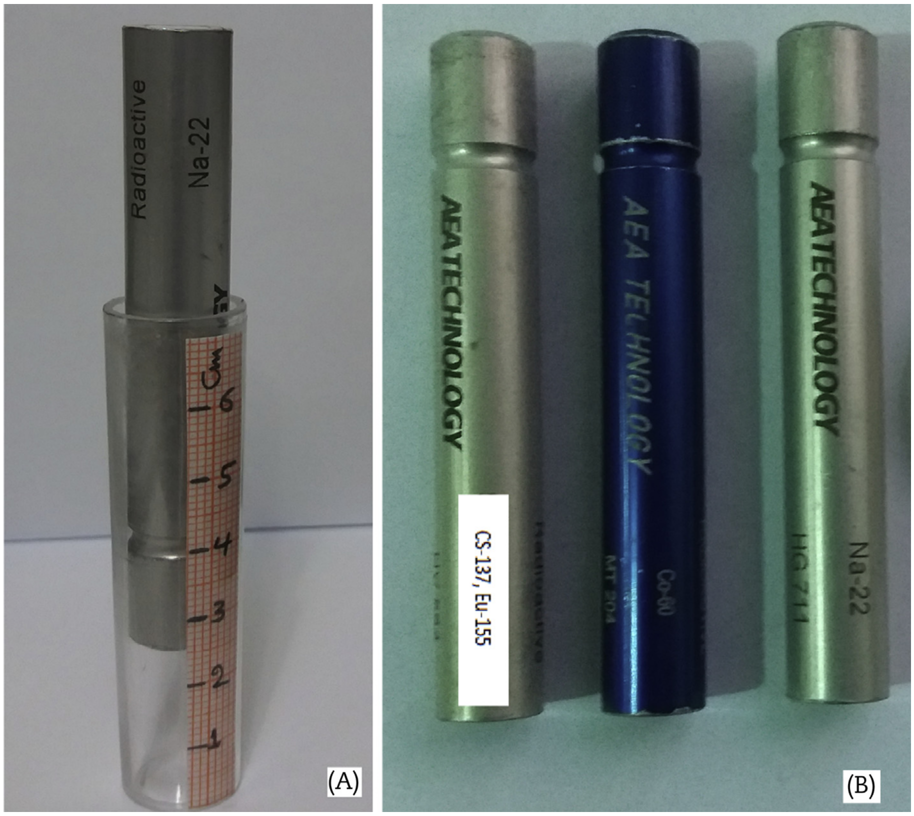

Fig. 3. (A) Marked glass tube. (B) Radioactive point sources.

The lower Pb segment has a small central hole of 5 cm diameter to hold the detector inside the shield. The photomultiplier tube, which passes through the hole, is covered by a thin plastic sheet, as recommended, to avoid direct shield–detector contact and to reduce the electrical signal noise produced by the shield. A photograph of the detector and shield is shown in Fig. 1.

The crystal of the detector stands inside a cylindrical Pb shield with wall thickness of 6 cm. The detector is covered on the inside with a thin sheet of Cu. Photomultiplier and preamplifier stand outside the cylindrical Pb shield.

2.2. NaI(Tl) detector characterization

The $3'' \times 3''$ NaI(Tl) well-type detector model, 3S3W, SILENA USA, shown in Fig. 1A, is used for measurements. The detector contains a high resolution NaI(Tl) crystal, a photomultiplier tube, an inner magnetic light shield, an aluminum cover, and a 14-pin connector. The manufacturer's drawing of the detector and information on the detector arrangement parameters are presented in Fig. 2. The 3S3W series of NaI(Tl) detectors can provide high efficiency and homogeneous response on both the cylindrical and well configurations, with long-term reliability and constancy. The Model 3S3W assembly is plugged directly into the tube base, which provides power for the photomultiplier tube [12]. The spectra are acquired and analyzed using A65-BW MAESTRO Multi Channel Analyzer (MCA) application software, by Ortec Company (Illinois Ave Oak Ridge, USA). The amplifier is a Canberra spectroscopy amplifier Model 2007P, operated with the settings of gain = 1.2 and shaping time = 0.75 μs, and operated under a high voltage of 820V.

Table 1
The energies, half-life, emission probabilities, and present activities of the radioisotope sources.

Nuclide	Energy (keV)	Half-life (day)	Emission probability (%)	Activity (kBq)
^{155}Eu	86.5	1736	30.7	0.649
	105.3		21.1	
^{137}Cs	662	10990	85	235.3
^{60}Co	1173	1925.23	99.85	24.5
	1333		99.98	
^{22}Na	511	950.57	180	1.182
	1274		100	

2.3. Energy and efficiency calibration

The energy and efficiency calibration of the MCA using standard sources is a procedure periodically performed for the NaI(Tl) detector.

Energy calibration of the γ-ray spectrometer establishes a relationship between the channel number of the MCA and the γ-ray energy (pulse height), which is essential for γ-ray spectrum analysis. Standard International Atomic Energy Agency sources were used for this calibration.

As in energy calibration, the same multisource gamma ray standard sources are used to determine detector efficiency. After identification of photopeak energies with the corresponding channel numbers of standard sources, the efficiency value is calculated taking into account the probability of disintegration ($f\gamma$) of each energy source established in various positions from 0.5 to 6 cm height inside the well in steps of 0.5 cm. The peak efficiency for the NaI(Tl) detector was obtained using the following equation for each gamma ray emitted by the radionuclide sources used [13,14].

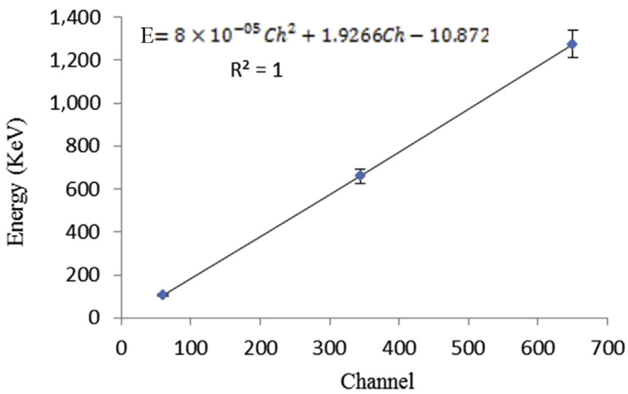

Fig. 4. Energy spectrum and calibration fit for ^{155}Eu, ^{137}Cs, and ^{22}Na sources.

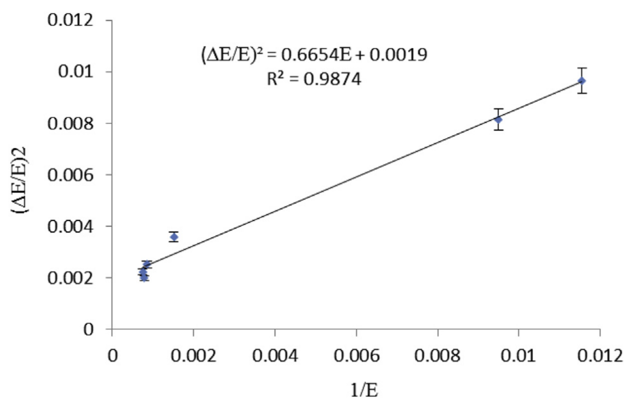

Fig. 5. Energy resolution of the well-type NaI(Tl) detector obtained for 2.5 cm height inside the well.

$$\varepsilon = \frac{N}{A \times t \times f_\gamma} \times 100\% \tag{1}$$

where N is the net peak area obtained for each photopeak using the convenient fit function for the NaI (Tl) detector. The live time t is the time during which the spectrum was acquired. A is the activity value of each radioisotope source at the time of measurement. fγ is the probability of gamma disintegration of the radionuclide.

As shown in Fig. 3, a marked glass tube is used to hold a point source; marks indicate source depth in the well. The three radioactive point sources were measured at 10 different heights inside and two different heights outside the well-detector. These sources are AEA technology Inc. Burlington, USA. The efficiency measurement was done for a period of 600 sec to obtain good statistics in the evaluation of each gamma peak; the counting electronics included a pile-up rejection circuit and a live time clock that was used for the dead time correction. The three radioactive point sources adopted are ^{155}Eu and ^{137}Cs, ^{60}Co, and ^{22}Na isotopes. Table 1 shows the energies, half-lives, emission probabilities, and present activity (at a time of measurements) of each radioisotope source [15].

3. Results and discussion

3.1. Energy and resolution calibrations

Energy and resolution calibrations are essential in gamma spectroscopy before its use in radiation detection.

The detector system should be calibrated for energy to convert channel number to energy scale. This calibration is carried out under laboratory conditions that mimic, as closely as possible, the experimental conditions. Several radioactive sources (at least 3 different energy peaks) are used to obtain certain photopeaks and to determine the channel number. This is usually done using ^{155}Eu, ^{37}Cs, and ^{22}Na standard gamma sources because they emit γ-ray energy of 105.3, 662, and 1274 KeV, respectively. In Fig. 4, the γ-ray spectrum obtained from those sources and a related quadratic fitting has been displayed. The energy calibration fitting gate is:

$$E = 8 \times 10^{-05} Ch^2 + 1.9266 Ch - 10.872 \;\; \text{With } R^2 = 1 \tag{2}$$

As can be seen, the relationship is very close to linear fitting.

The energy resolution of the detector system has a photopeak Gaussian distribution. The centroid represents the central value; and the full width at half maximum (FWHM) represents its width at half of the counts associated with the centroid value. The FWHM (ΔE) is known for its proportional relationship to the standard deviation, which is 2.36σ. Resolution calibration is useful to ensure that all photopeak areas are correctly measured. Fractional energy resolution is a linear proportionality equation between the centroid (E) and the ($[\Delta E]^2/E$) [1,16]. The resolution equation can be determined using ^{155}Eu, ^{22}Na, ^{60}Co, and ^{137}Cs gamma standard sources

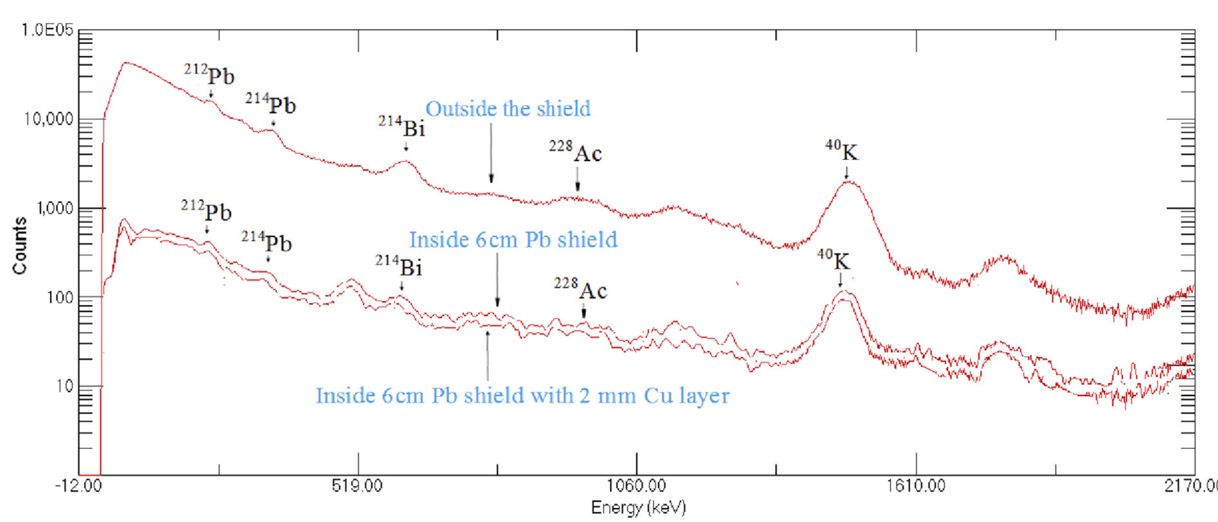

Fig. 6. The 3″ × 3″ well type NaI(Tl) background spectrum without the shield, inside the 6 cm Pb shield and inside the 6 cm Pb with 2 mm Cu layer (log scale).

Table 2
Background counts and spectra ratios without shield, inside the Pb shield and inside Pb with Cu layer.

Source/energy keV	Outside the shield (I_{out})	Inside the Pb shield (I_{in1})	Inside the Pb shield with 2 mm Cu (I_{in2})	I_{out}/I_{in1}	I_{out}/I_{in2}	I_{in1}/I_{in2}
(20–2160 keV)	4069000 ± 3780	142000 ± 1050	140000 ± 1150	28.65	29.06	1.01
(20–500 keV)	3100000 ± 3990	74000 ± 1020	71000 ± 950	41.89	43.66	1.04
^{212}Pb (238.63)	18800 ± 860	490 ± 145	400 ± 140	38.37	47.00	1.26
^{214}Pb (351.93)	15005 ± 680	420 ± 165	390 ± 185	35.73	38.47	1.08
^{214}Bi (609.3)	3390 ± 380	181 ± 80	181 ± 70	18.70	18.70	1.00
^{228}Ac (911.21)	1322 ± 320	111 ± 60	111 ± 54	11.90	11.90	1.00
^{40}K (1460.8)	1812 ± 260	122 ± 80	115 ± 70	14.85	15.76	1.06

Table 3
Comparison of background spectra ratio of the present work with other works.

Source/Energy KeV	3″×3″ NaI(TI) 6cm Pb present work		9″×9″ NaI(Tl) 15cm Pb [3]	HPGe 12cm Pb [2]	
	$I_{out/in1}$	I_{out}/I_{in2}	I_{out}/I_{in}	I_{out}/I_{in1}	$I_{out/PbCuN2}$
^{232}Th/^{212}Pb (238.63)	38.37	47.00	–	10.0	10.0
^{238}U/^{214}Pb (351.93)	35.73	38.47	–	3.0	>7.7
^{238}U/^{214}Bi (609.3)	18.70	18.70	191.2	5.6	>12.5
^{232}Th/^{228}Ac (911.21)	11.90	11.90	–	>10.0	>10.0
^{40}K (1460.8)	14.85	15.76	97.3	9.1	12.5

and modeled by EXCEL. The FWHM of the NaI(Tl) detector increases with increasing gamma ray energy, as can be seen in Fig. 5.

It is worthwhile to mention that the energy calibration and the resolution of any single energy line are independent of the locations of the γ-source inside or outside of the well.

3.2. Effect of Pb and Cu shielding

To show the effect of Pb gamma shielding and the Cu sheet on X-rays produced by the Pb shield, three cases of measurement were carried out. In the first case, a bar detector without any shielding was used; in the second case, the detector was brought into the 6 cm Pb shield; in the final case, the detector was covered with 2 mm of Cu inside 6 cm of Pb shield; these three cases are compared using counts in log scale and with a marked 1460.8 KeV line (^{40}K). All spectra numbers on the y-axes represent counts for 15000 sec live time measurements while numbers on the x-axes are the gamma-line energies in KeV. Fig. 6 shows the spectra of the 3″ × 3″ well-type NaI(Tl) detector for the three cases.

In Table 2, the ratios between the background spectra, without the shield I_{out}, with Pb alone (I_{in1}), and with both Pb and Cu (I_{in2}) shields, are given. As is shown in the fifth column of Table 2, (I_{out}/I_{in1}), the low energy lines inside the shield are reduced more than 35 times. The reduction decreases to less than 19 times at higher energy lines up to the line of ^{40}K (1460.8 KeV), where the reduction increased a little bit again to 15 times which might be because of the sum of the lower energies. The total count (20 KeV–2160 KeV) is reduced about 29 times, which perfectly agrees with the above energy line reduction behaviors.

Columns 6 and 7 of Table 2 show the effects of adding 2 mm Cu covering to the detector inside the Pb shield. It is very clear that there is a dominant effect on low-energy particles, while there is negligible effect on higher energy particles.

Comparisons of the present work (6 cm Pb and 2 mm Cu shield) with other work achieved in the University of Novi Sad, Serbia, using a 9″ × 9″ NaI(Tl) with 15 cm Pb shield [3], and with an High Purity Germanium (HPGe) detector with 12 cm Pb (I_{in1}) shield and Pb, Sn, and Cu (I_{PbCuN2}) and without the shield (I_{out}) [2] are given in Table 3. It can be observed that the reduction of the 15 cm Pb 9″ × 9″ NaI(Tl) is about 10-fold higher than that of the 6 cm (present work) device, while the present results are comparable to those shown for the HPGe detector.

3.3. Detector efficiency calculation

The detection efficiency of the NaI(Tl) detector is obtained directly from the ^{137}Cs and ^{22}Na (1274 KeV) isotopes by using Equation 1 for each gamma ray photopeak energy. For ^{155}Eu and ^{60}Co, the calculations are based on the transfer method presented in the study by Abdullah [16], used to determine the doublet photopeak area. Among those sources, at position 2.5 cm inside the well, a typical gamma-ray spectrum of ^{22}Na, captured from the software, is given in Fig. 7. These measurements are done when the sources are placed at a midpoint of the well (i.e., at 2.5 cm from the well bottom). As was expected, the detector efficiency decreased

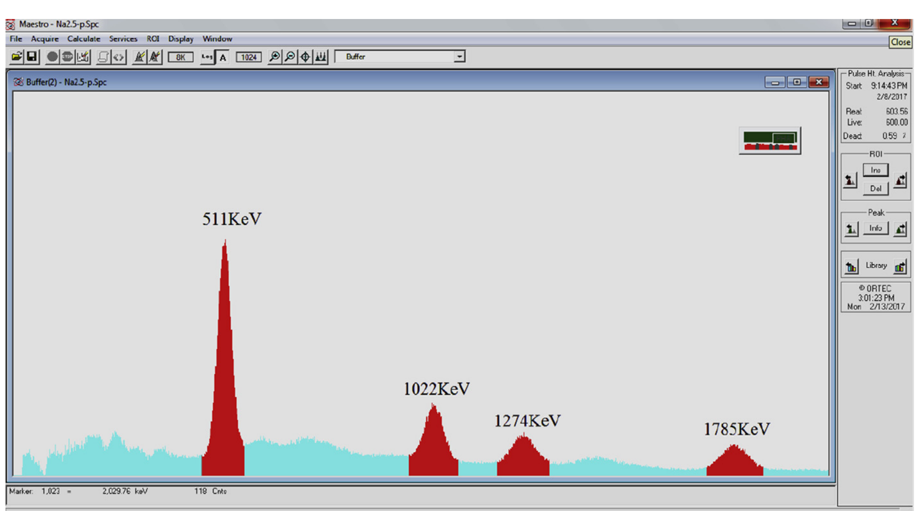

Fig. 7. Gamma-ray spectrum obtained from ^{22}Na source (at 2.5 cm).

Table 4
Detector efficiency calculation.

Source	Energy (E) KeV	Efficiency % present work	Efficiency % 9″ × 9″NaI(Tl) [7]
^{155}Eu	86.5	34 ± 0.251	–
^{155}Eu	105	33.34 ± 0.322	–
^{137}Cs	662	15 ± 0.007	–
^{60}Co	1173	4.23 ± 0.013	11.5
^{22}Na	1274	2.95 ± 0.072	5
^{60}Co	1333	3.5 ± 0.012	10

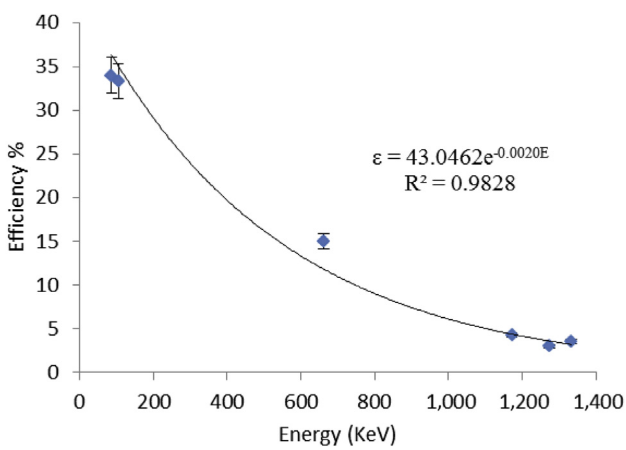

Fig. 8. Detection efficiency of 3″ × 3″ well-type NaI(Tl) detector as a function of gamma-ray energies (source placed at 2.5 cm height inside the well).

with increasing energy, as shown in Table 4. The obtained results are plotted using the EXCEL program and have been displayed as a function of gamma ray energy in Fig. 8. As can be seen in this figure, there is a great variety of analytical functions that can be used to describe the dependence of the efficiency on the energy. The solid line represents an exponential fit of efficiency $\varepsilon = 43.0462e^{-0.002E}$ to the resulting points; the line gives a good description, with a correlation coefficient of $R^2 = 0.9828$ between the efficiency and the gamma-ray energies (E).

The present results have been compared with those obtained using the 9″ × 9″ well-type NaI(Tl) detector. For comparison, the midpoint (9 cm) inside the well is considered. It is observed that the detector efficiency approximately doubled, as given in column 4 of Table 4. Also a good agreement of the efficiency behavior for all energy lines or variation with the depth of the well is obtained [7].

Because the detection efficiency of the NaI(Tl) detector varies with the depth of the detector well, the efficiencies were obtained for different heights from the bottom inside the detector well for the full shielding case. The results are displayed in Fig. 9 for 12 different heights and nine different photopeak energy lines.

The simplest case is with ^{137}Cs with only one gamma line (662 KeV). The efficiency is largest when the point source is deep inside the detector well; efficiency decreases gradually with the height positions of the point source, as shown in Fig. 9A.

The efficiency for the ^{60}Co gamma lines (1173 KeV and 1333 KeV) first remains almost constant from the bottom to 2.5 cm height; it then remarkably decreases. Even after the point source is out of the detector well (after height of 5 cm) for one centimeter, the decrease remains the same as in the upper half the detector well, as shown in Fig. 9B.

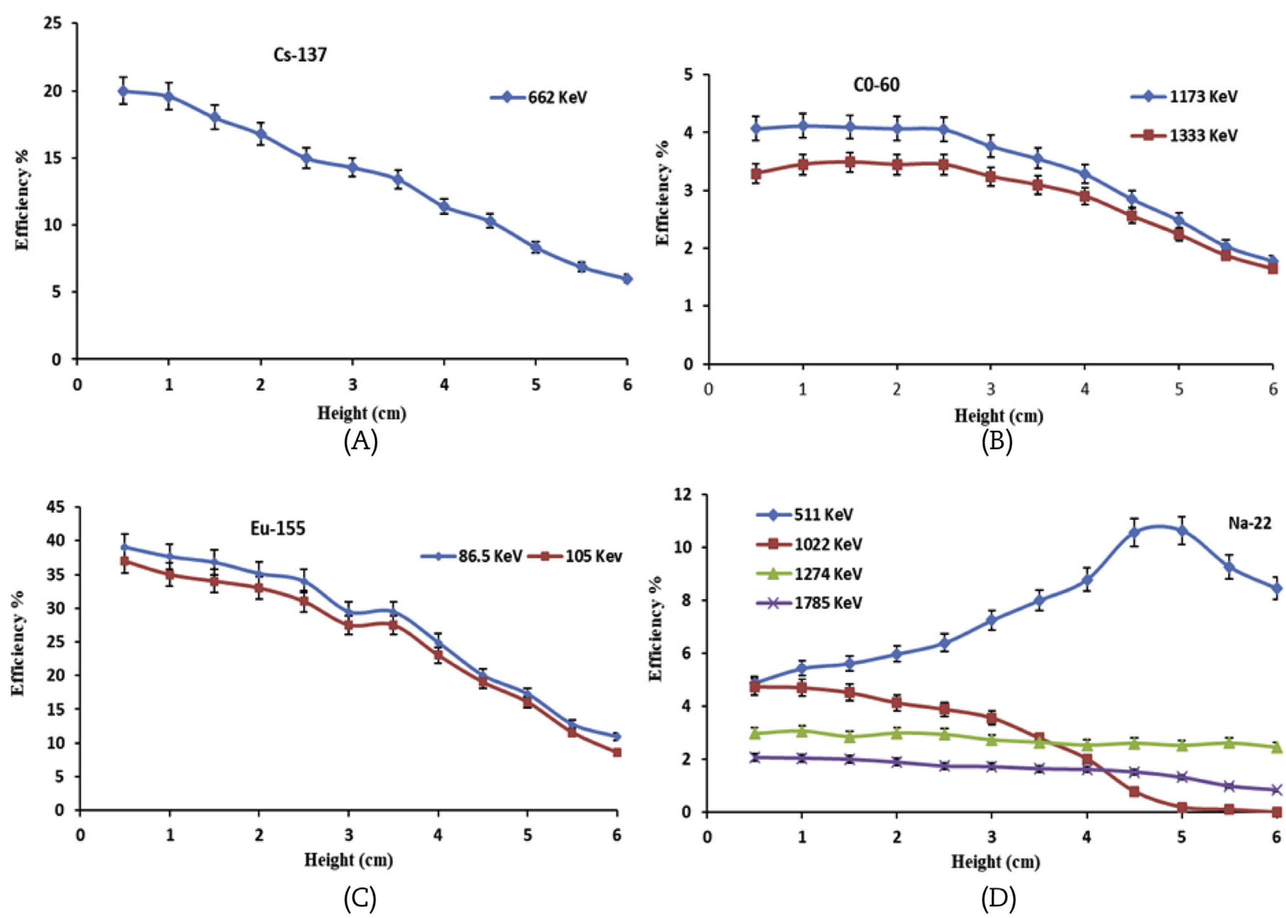

Fig. 9. Well detector peak efficiency dependence as a function of position height. (A) ^{137}Cs. (B) ^{60}Co. (C) ^{155}Eu. (D) ^{22}Na point sources.

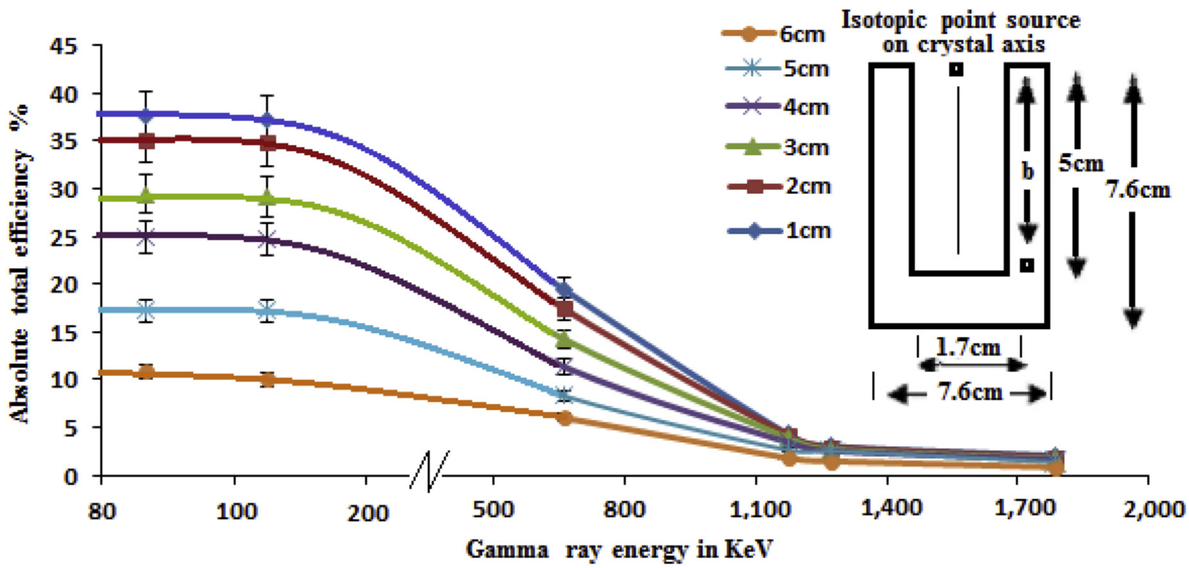

Fig. 10. Experimental absolute efficiency measured by a point gamma-ray sources 86.5 KeV, 105 KeV, 662 KeV, 1274 KeV and 1785 KeV for a 3″ × 3″ NaI(Tl) well-type scintillation as a function of the source location.

^{155}Eu emits two gammas (86.5 KeVand105.3 KeV): their behaviors are almost identical to the gamma line of ^{60}Co, here with low decreases with height. The highest efficiency and probability for summing is deep inside the detector well and decreases with the position height of the point source, as shown in Fig. 9C.

The most complex case is of ^{22}Na, for which the spectrum contains the 511 KeV gamma line and the 1274 KeV gamma line. Additional lines can be found at 1022 KeV (2 × 511 KeV) and 1785 KeV, the sum of (gamma + 511 KeV). Results of efficiency dependency on position height of point source are presented in Fig. 9D.

The efficiency of the 511 KeV line increases slowly with the height of the point source until a height of 5 cm (surface of the detector). Unsurprisingly, after the point source is out of the detector, the efficiency for 511 KeV practically decreases with the distance from the surface, obeying the inverse square law.

The efficiency for the 1022 KeV (2 × 511 KeV) line decreases to zero outside the detector well because annihilation quanta are emitted in opposite directions.

Interesting is that the efficiency of the gamma line at 1274 KeV is relatively constant and insensitive to the position height of the point source. That this might be because a lowering of the geometrical efficiency of the 1274 KeV gamma line is compensated for by a lowering of the (true and random) summing-out effects with annihilation photons and random summing with other 1274 KeV gammas [7]. On the other hand, the behavior of the 1785 KeV line, which is the sum of gamma + 511 KeV is practically constant until the surface of the detector.

Unlike Fig. 9, Fig 10 summarizes the detection efficiencies of the photopeak energies of the four (^{155}Eu, ^{137}Cs, ^{60}Co, and ^{22}Na) radioisotopes as a function of energy for all depths of the detector well; it can be seen in this figure that the detection efficiency decreases with increasing distance from the bottom of the detector well, as had been expected [17]. Also the efficiency at the bottom is more than double that at the surface.

4. Conclusion

The designed Pb shield exhibited very good performance. It seems that adding a thin sheet of Cu is a good choice to reduce the low gamma energies and X-rays produced by the interaction of high gamma energies with Pb. Hopefully, with the addition of Cu, the gamma-spectrometry laboratory will be even more efficient in low-level radioactivity measurements of environmental samples. It is also interesting to mention that no traces of any contamination in the shielding materials were found.

Concerning the efficiency of the utilized detector, it is clear that the detector response directly depends on the position and energy of the point source.

The spectrum and the results are very simple for a relatively weak radioactive source, as in ^{155}Eu, much more complicated spectrum exist when sources have relatively larger count rates, as in ^{22}Na.

The process of annihilation, $e^- + e^+ \rightarrow 2\gamma$ produces photons of equal energy, back-to-back in the laboratory, i.e. 180° strong angular dependency. This means that the detector absorbs and records 1022 keV lines more than the 511 keV photons whenever the source sinks inside the depth of the well more and more. This is very clear in the efficiency of the two 511 keV emitting photons from ^{22}Na radioactive source.

The energy calibrations for all energy lines, as well as, the resolution of any energy line are independent on the locations of the γ-source inside or outside of the well.

Conflict of interest

The authors have no conflict of interest to declare.

References

[1] I. Akkurt, K. Gunoglu, S.S. Arda, Detection Efficiency of NaI (Tl) Detector in 511 – 1332 keV Energy Range, Sci. Technol. Nucl. Install. 2014 (2014) 6–11.
[2] D.S. Mrd, I.S. Bikit, I.V. Anicin, J.M. Slivka, J.J. Hansman, N.M. Zikic-Todorovic, E.Z. Varga, S.M. Curcic, J.M. Puzovi, Background reduction using Fe and Pb shielding, J. Res. Phys. 30 (2004) 49–54.
[3] J. Hansman, Design and construction of a shield for the 9″ × 9″ NaI(Tl) well-type detector, Nucl. Technol. Radiat. Prot. 29 (2014) 165–169.
[4] A. Jehouani, R. Ichaoui, M. Boulkheir, Study of the NaI(Tl) efficiency by Monte Carlo method, Appl. Radiat. Isot. 53 (2000) 887–891.
[5] S. Sen, A. Chandra, D. Pramanik, M.S. Sarkar, Study of Intrinsic Photo peak Efficiency of NaI (Tl) Detectors at 662 KeV, Proceeding DAE Symo, Nucl. Phys. 58 (2013) 934–935.

[6] M.S. Badawi, M. Abd-Elzaher, A.A. Thabet, A.M. El-Khatib, An empirical formula to calculate the full energy peak efficiency of scintillation detectors, Appl. Radiat. Isot. 74 (2013) 46–49.
[7] J. Hansman, D. Mrdja, J. Slivka, M. Krmar, I. Bikit, Efficiency study of a big volume well type NaI(Tl) detector by point and voluminous sources and Monte-Carlo simulation, Appl. Radiat. Isot. 99 (2015) 150–154.
[8] M.I. Abbas, Analytical formulae for well-type NaI (Tl) and HPGe detectors efficiency computation, Appl. Radiat. Isot. 55 (2001) 245–252.
[9] S. Yalcin, O. Gurler, G. Kaynak, O. Gundogdu, Calculation of total counting efficiency of a NaI(Tl) detector by hybrid Monte-Carlo method for point and disk sources, Appl. Radiat. Isot. 65 (2007) 1179–1186.
[10] G.A. Brinkman, A.H.W. Aten, J.T. Veenboer, Absolute Standardization with a NaI(Tl) Crystal - I Calibration by Means of a Single Nuclide, Int. J. Appl. Radiat. Isot. 14 (1963) 153–157.
[11] F. Cejnar, I. Kovář, Experimental and calculated photopeak efficiency values for well-type NaI(Tl) detectors, Int. J. Appl. Radiat. Isot. 31 (1980) 79–84.
[12] Silena international S.P.A web page, 2016. http://www.geocities.ws/silenaspa/silena/profile.htm.
[13] K.M.S. Abdullah, R.A. Ramadhan, Determination of Gamma-Emitting Radionuclides in Duhok City, Iraq, Nuclear 48 (2011) 295–300.
[14] D. Demir, A. Un, Y. Sahin, Efficiency determination for NaI (Tl) detectors in the 23 keV to 1333 keV energy range, Instrum. Sci. Technol. 36 (2008) 291–301.
[15] G. Gilmore, Practical Gamma-ray Spectrometry, second ed., John Wiley & Sons Ltd, 2008.
[16] K.M.S. Abdullah, A Method to Determine Doublet Photopeak Area ^{137}Cs and ^{214}Bi, in NORM Soil by NaI-detector, Int, J. Fundam. Phys. Sci 5 (2015) 32–37.
[17] G.F. Knoll, Radiation Detection and Measurement, third ed., John Wiley & Sons, Inc., 2000.